

Breast Lesions: Quantitative Elastography with Supersonic Shear Imaging—Preliminary Results¹

Alexandra Athanasiou, MD
Anne Tardivon, MD
Mickael Tanter, PhD
Brigitte Sigal-Zafrani, MD
Jeremy Bercoff, PhD
Thomas Deffieux, PhD
Jean-Luc Gennisson, PhD
Mathias Fink, PhD
Sylvia Neuenschwander, MD

Purpose:

To determine the appearance of breast lesions at quantitative ultrasonographic (US) elastography by using supersonic shear imaging (SSI) and to assess the correlation between quantitative values of lesion stiffness and pathologic results, which were used as the reference standard.

Materials and Methods:

This study was approved by the French National Committee for the Protection of Patients Participating in Biomedical Research Programs. All patients provided written informed consent. Conventional US and SSI quantitative elastography were performed in 46 women (mean age, 57.6 years; age range, 38–71 years) with 48 breast lesions (28 benign, 20 malignant; mean size, 14.7 mm); pathologic results were available in all cases. Quantitative lesion elasticity was measured in terms of the Young modulus (in kilopascals). Sensitivity, specificity, and area under the curve were obtained by using a receiver operating characteristic curve analysis to assess diagnostic performance.

Results:

All breast lesions were detected at SSI. Malignant lesions exhibited a mean elasticity value of $146.6 \text{ kPa} \pm 40.05$ (standard deviation), whereas benign ones had an elasticity value of $45.3 \text{ kPa} \pm 41.1$ ($P < .001$). Complicated cysts were differentiated from solid lesions because they had elasticity values of 0 kPa (no signal was retrieved from liquid areas).

Conclusion:

SSI provides quantitative elasticity measurements, thus adding complementary information that potentially could help in breast lesion characterization with B-mode US.

© RSNA, 2010

¹ From the Departments of Radiology (A.A., A.T., S.N.) and Tumor Biology (B.S.), Institut Curie, 26 rue d'Ulm, 752048 Paris Cedex 05, France; Laboratoire Ondes et Acoustique, Centre National de Recherche Scientifique, Unité Mixte de Recherche 7587, Ecole Supérieure de Physique et Chimie Industrielle, Paris, France (M.T., T.D., J.L.G., M.F.); and SuperSonic Imagine, Aix-en-Provence, France (J.B.). Received March 3, 2009; revision requested April 13; final revision received August 14; accepted September 4; final version accepted February 3, 2010. Address correspondence to A.A. (e-mail: alexandra.athanasiou@curie.net).

© RSNA, 2010

Palpation is a standard medical practice relying on qualitative estimation of tissue Young modulus $E = \sigma/\epsilon$, where σ is the external compression (stress) and ϵ is the deformation of the tissue because of this compression (strain). Generally, benign lesions tend to be harder than normal breast tissue but softer than cancers (1). Exceptions can occur, but soft malignant lesions, including medullary, mucinous, papillary, and some necrotic infiltrating ductal carcinomas, are uncommon (2). On the other hand, some benign lesions, such as hyalinized fibroadenomas and fat necrosis, can be hard at palpation. At B-mode ultrasonography (US), there is no correlation between the lesion's echo pattern and the Young modulus; hard and soft lesions may exhibit similar echogenicity. Elastography has emerged as a promising technique for improving lesion differentiation. It can be used to estimate breast tissue elasticity by measuring tissue strain or tissue displacement during sonologist-induced mechanical excitation (3). The principle applied is that strain will be less in harder tissue. Some currently available US systems include a strain imaging software package: strain images, usually color coded, are displayed in real time as the user applies light compression on breast tissue with the transducer. With freehand compression, the influence of probe

movement has certain disadvantages: the elasticity map obtained is highly dependent on the organ's compressibility limits under stress and on the extent of tissue compression applied. The displayed information is about local strain estimated at a given location in tissues, but it depends on surrounding mechanical properties and it is not quantitative. Despite these caveats, the value of this technique in the evaluation of breast lesions already has been reported (4–8).

To overcome this problem, we developed a quantitative elastography technique, supersonic shear imaging (SSI), that combines two concepts. Instead of using mechanical external compression, the system itself remotely induces mechanical vibration by using acoustic radiation force created by a focused ultrasound beam. A very fast (5000 frames per second) US acquisition sequence is used to capture the propagation of shear waves. Both steps are performed by using the same conventional US probe (9–12). The displacement induced at the focus (for example, a breast lesion) generates a shear wave that conveys information linked to the local viscoelastic properties of the tissue, thus enabling a quantitative approach to elasticity values. The shear wave speed v is linked with shear modulus μ by the equation $\mu = \rho v^2$, where ρ is the local density (constant and equal to 1000 $\text{kg} \cdot \text{m}^{-3}$ in soft tissues). In soft tissues, local stiffness is described by the Young modulus E and can be approximated by $E \approx 3\mu$ (13). With imaging in real time, the propagation of the shear wave enables the recovery of local shear wave

speed and, consequently, the mapping of local tissue stiffness. Our purpose was to determine the appearance of breast lesions at quantitative US elastography by using SSI and to assess the correlation between quantitative values of lesion stiffness and pathologic results, which were used as the reference standard.

Materials and Methods

The patent holder for this technique is Laboratoire Ondes et Acoustique, Ecole Supérieure de Physique et Chimie Industrielle (Paris, France), where M.T., T.D., J.L.G., and M.F. are employees. M.T. is a cofounder of and shareholder in, J.B. is a founder of, and M.F. is a shareholder in and scientific adviser to SuperSonic Imagine (Aix-en-Provence, France), which provided the equipment and the technical support for the study (programming of US sequences and data postprocessing). Data were controlled by authors (A.A. and A.T.) who do not have any financial interest.

Patients

This study was approved by the French National Committee for the Protection of Patients Participating in Biomedical Research Programs. All patients provided written informed consent. We performed SSI in 62 consecutive women with mammographically occult lesions seen only at US who were referred to the Curie Institute (Paris,

Advances in Knowledge

- Supersonic shear imaging (SSI) elastography can improve differentiation of solid from atypical B-mode cystic breast lesions (manifesting as hypoechoic lesions) because no signal is retrieved from liquid areas (atypical cyst elasticity value, 0 kPa).
- No external mechanical compression is needed with SSI elastography, which is based on the mechanical excitation that interrogates breast tissue mechanical properties by means of remote palpation induced by the radiation force of ultrasound beams transmitted by a conventional US probe.

Implications for Patient Care

- The addition of the elasticity parameter in the overall Breast Imaging Reporting and Data System classification potentially could improve the specificity of breast US.
- The detection of cystic lesions potentially could reduce the number of fine-needle aspiration biopsies performed for proteinaceous or hemorrhagic cysts that have an atypical B-mode appearance.

Published online before print

10.1148/radiol.10090385

Radiology 2010; 256:297–303

Abbreviations:

BI-RADS = Breast Imaging Reporting and Data System
SSI = supersonic shear imaging

Author contributions:

Guarantors of integrity of entire study, A.A., J.L.G.; study concepts/study design or data acquisition or data analysis/interpretation, all authors; manuscript drafting or manuscript revision for important intellectual content, all authors; manuscript final version approval, all authors; literature research, A.A., M.T., B.S., T.D., J.L.G., M.F., S.N.; clinical studies, A.A., A.T., M.T., B.S., J.B., T.D., J.L.G.; statistical analysis, M.T., J.L.G.; and manuscript editing, A.A., A.T., M.T., B.S., J.B., J.L.G., S.N.

See Materials and Methods for pertinent disclosures.

France) between September 2006 and March 2007 for evaluation and percutaneous procedures. Twelve patients were excluded because of technical hardware problems during SSI acquisition; the prototype power supply encountered a stability problem, and no raw US data were acquired for these patients. Four patients refused to undergo a percutaneous interventional procedure and were excluded because of lack of pathologic result. Final analysis was based on data in 46 patients (mean age, 57.6 years; age range, 38–71 years) who had 48 nonpalpable breast lesions (7–16 mm; mean size, $14.7 \text{ mm} \pm 1.3$ [standard deviation]) detected at US. Six lesions were classified as Breast Imaging Reporting and Data System (BI-RADS) 3; 28 lesions, as BI-RADS 4; and 14 lesions, as BI-RADS 5. Percutaneous procedures for BI-RADS 3 lesions were performed in patients at high risk.

Imaging Workflow

Lesions were depicted at B-mode US by using the hospital US system (Aplio XG, model SSA-790 A; Toshiba Medical Systems Europe, Zoetermeer, the Netherlands) equipped with a 12-MHz probe. Patients originally underwent scanning performed together by A.A. and A.T. (radiologists specialized in breast imaging, with 8 and 15 years of experience, respectively) for clinical indications. Mammograms were available in all cases, but lesions were mammographically occult because of either small size or dense breast parenchyma. Lesion location, size, echo pattern, and BI-RADS classification (14) were noted. The BI-RADS score was recorded by means of consensus by A.A. and A.T.

SSI sequences were performed by using a modified system (ATL HDI 1000; Philips Medical Systems, Best, the Netherlands) with a linear array (L7-4; Philips Medical Systems). The system was reprogrammed to provide, in addition to its standard capabilities, a special SSI acquisition mode by means of button activation. All safety considerations were satisfied according to the U.S. Food and Drug Administration (15). The highest values recorded for our prototype were as follows: mechanical index, 1.4

(<1.9); spatial-peak temporal-average intensity, 603 mW/cm^2 (< 720 mW/cm^2); and thermal index, 0.48 (<6). Spatial-peak temporal-average intensity and thermal index were calculated by assuming a 1-Hz SSI frame rate, which was much lower in practice because two successive acquisitions were launched with a pause of 5 to 10 seconds.

The radiologist (A.A., A.T.) performing the SSI first obtained B-mode images that were saved on the system hard drive (36×44 -mm rectangular window). For each lesion, two SSI sequences were performed; each sequence comprised three successive pushing beams. During the first sequence, the radiologist located the lesion in the center of the screen. The first pushing beam was centered along the central axis of the lesion; the second, on the right side of the lesion; and the third, on the left side of the lesion. Each pushing beam lasted about 3 seconds, and three pushing beams were necessary to produce a full elastography image (12). During the second SSI sequence, the radiologist located the lesion on the left or the right side of the screen to have both the lesion and surrounding parenchyma on the screen; the three pushing beams were used to obtain a full elastography image of both the lesion and the parenchyma.

The total time of the SSI examination was less than 5 minutes. Examination results were transferred to an off-line computer by using an Ethernet cable limited to a 1 Mb/sec transfer rate and were processed with dedicated elastography software. Postprocessing time was 5 seconds for each quantitative elasticity image. The accuracy of SSI values was compared previously with calibrated phantoms in other studies ($\pm 8\%$ error margin) (16). US-guided procedures were then performed during the same session by using the hospital US system.

Elastography Sequence and Data Processing

Each SSI sequence corresponded to the generation of a vibration force by means of successively focusing ultrasound beams at five different depths. Each pushing focused beam consisted

of a 150- μsec burst at 5 MHz. Successive focusing depths were separated by 5 mm, making the pushing line 30 mm long. This supersonic source generated plane shear waves that propagated transversally in tissue in a few tens of milliseconds. These shear waves were imaged by means of a very fast imaging sequence; 60 flat insonications (5-MHz burst of 1 μsec) were performed at a 4000-Hz pulse repetition frequency. Raw radiofrequency data corresponding to back-scattered echoes were recorded and stored. The imaging sequence provided a US video of the tissue during shear wave propagation. On the basis of this video, displacements induced by the shear wave in tissues were calculated by comparing US frames by using classic speckle-tracking algorithms. Shear wave propagation speed then was deduced locally by using a one-dimensional cross-correlation algorithm to estimate the time shift between the two temporal displacement signals separated by 1 mm. Finally, the local Young modulus E was deduced.

Elasticity maps deduced from each of three acquisitions, corresponding to three different pushing lines, were then merged to compute the final elasticity map that covered the entire width of the US image. The result was displayed on a color scale ranging from 0 to 240 kPa; the corresponding shear wave speed thus roughly ranged from 0 to 8 m/sec. Spatial resolution was 1 mm^2 .

Data Analysis

Lesion dimensions were measured by using calipers on recorded B-mode US images obtained with the hospital system and SSI postacquisition images. Two quantitative elasticity values were extracted, the first corresponding to the elasticity value of the lesion and the second to the elasticity value of normal tissue. Two 3×3 -mm boxes were positioned, one box in the lesion area at the location of maximum stiffness and one in normal-appearing tissue (glandular and fatty tissue, which was distinguished by its lobular form, compressibility, and low echogenicity), by A.A. and A.T. together. Cystic lesions were

not used for the estimation of average values because cysts do not have a stiffness value ($E = 0$ kPa). The whole procedure lasted about 5 minutes.

Pathologic Examination

Twenty-eight lesions were benign at percutaneous US-guided biopsy ($n = 16$) or fine-needle aspiration ($n = 12$) (Table); no further surgery was performed except in one lesion that corresponded to a grade I phyllodes tumor. Seven lesions corresponded to cysts (four had a proteinaceous or hemorrhagic component). Twenty lesions were malignant at biopsy, and further surgical excision was performed. Final histologic diagnosis and tumor grade were defined by using the surgical specimen. All diagnoses were made by a pathologist (B.S., with 18 years of experience in breast pathologic examination).

Statistical Analysis

The role of elasticity values in discriminating malignant from benign lesions was studied by using a nonparametric Mann-Whitney test. Receiver operating characteristic curves were used to compare the performance of estimators corresponding to the established BI-RADS variable and to a modified BI-RADS variable taking into account the lesion's mean Young modulus E , named β . Because the elasticity parameter is not envisioned as a stand-alone parameter but rather as an added value to US examination, the combination of the BI-RADS score with the Young modulus variable E was estimated. The distribution of E was rescaled, shifted to the interval $(-1, +1)$, and added linearly to the BI-RADS score. The rescaling process was based on the following equation: $\beta = \text{BI-RADS} + 2E/E_{\text{max}} - 1$, where β stands for the combined parameter BI-RADS + elasticity, which allows the SSI elasticity value to change the BI-RADS score by at most ± 1 unit. To shift elasticity to the interval $[-1, +1]$, we normalized each lesion elasticity value by comparing it to the maximum elasticity found during SSI imaging in the entire study population, defined as E_{max} . The elasticity value (E) was measured for each lesion and was then normalized by a factor of 2 ($2E/E_{\text{max}}$).

Final Pathologic Diagnosis in 48 Breast Lesions

Pathologic Diagnosis	No. of Lesions
Malignant lesions ($n = 20$)	
Infiltrating ductal carcinoma grade I	3
Infiltrating ductal carcinoma grade II	9*
Infiltrating ductal carcinoma grade III	5
Infiltrating lobular carcinoma grade III	2
Infiltrating mixed ductal and lobular carcinoma	1
Benign lesions ($n = 28$)	
Fibroadenoma	8
Aberrations of normal development and involution	9
Cyst	7
Benign grade I phyllodes tumor	1
Fat necrosis	2
Intramammary lymph node	1

* Includes one lesion with extensive intraductal component.

Then, -1 was added to the normalized score ($2E/E_{\text{max}} - 1$). Any value lower than $E_{\text{max}}/2$ would be given a score of -1 , and any value higher than the mean would be given a score of $+1$. Only values exactly equal to $E_{\text{max}}/2$ would be given a score of 0 . The value calculated was added to the BI-RADS score, thus modifying the BI-RADS score by 0 , -1 , or $+1$.

Areas under the curve were compared by using a Hanley and McNeil test (17). Sensitivity and specificity values and their respective 95% confidence intervals were estimated. $P < .05$ was considered to indicate a statistically significant difference. All data were analyzed by using software (MedCalc version 9.4.2.0; MedCalc Software, Mariakerke, Belgium).

Results

Normal Breast Tissue and Breast Cysts

Quantitative elasticity values in normal breast tissue clearly delineated the different structures. Fatty tissues displayed low values of elasticity (E , approximately 7 kPa), whereas breast parenchyma values ranged from 30 to 50 kPa (Fig 1). All breast cysts had elastography values of 0 (Fig 2).

Solid Lesions

Benign lesions had a mean elasticity value of $45.3 \text{ kPa} \pm 41.1$, whereas

malignant lesions demonstrated mean values of $146.6 \text{ kPa} \pm 40.05$ ($P < .001$) (Figs 3, 4).

Mean values of the new variable β were then compared by using the Mann-Whitney test, and they were also different ($P < .001$). The discriminating power for detection of malignancy of the variable β was significantly higher than that of the BI-RADS score alone, with an area under the receiver operating characteristic curve of 0.985 ± 0.01 (95% confidence interval: 0.884, 0.995) compared with the BI-RADS score area under the receiver operating characteristic curve of 0.917 ± 0.046 (95% confidence interval: 0.764, 0.968; $P < .05$) (Fig 5).

Comparison between receiver operating characteristic curves with a Hanley and McNeil test for BI-RADS and β gave a difference of 0.068 ± 0.033 ($P = .039$). The most important effect of the new variable β was for BI-RADS 4 lesions ($n = 28$). Adding the elasticity score modified the BI-RADS 4 score to BI-RADS 3 for 13 lesions, meaning that we could have avoided performing biopsy in 46% of cases and had a short 6-month follow-up instead. Nine of 28 BI-RADS 4 cases remained at the same score after the elasticity value was added, and six cases were recategorized as BI-RADS 5. No cancers were missed during this modification of BI-RADS score. The specificity of β

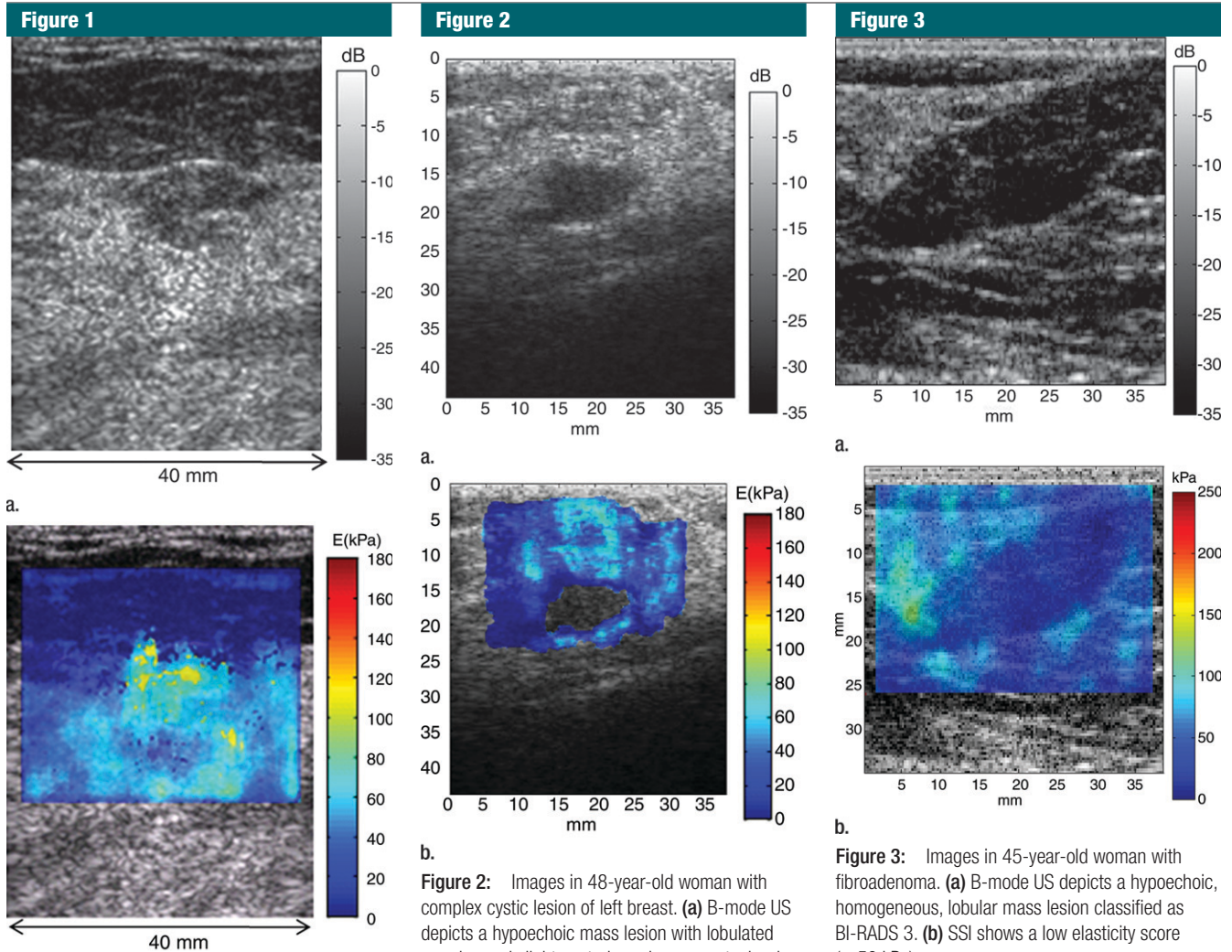


Figure 1: Normal breast tissue in 52-year-old woman. **(a)** B-mode US does not depict any particular lesion. **(b)** Elasticity map obtained by using SSI. The shear wave speed is coded on a color scale ranging from 0 to 8 m/sec, corresponding to a Young modulus ranging between 0 and 192 kPa. The elasticity map exhibits the delineation between soft fatty tissues (E , approximately 7 kPa) and breast parenchyma (E , approximately 30–50 kPa).

was 0.96, and the sensitivity was 0.95, whereas the specificity and sensitivity of the BI-RADS score were 0.63 and 0.96, respectively. No modification was noted in the BI-RADS 3 category. Only one BI-RADS 5 lesion was reduced to BI-RADS 4 according to the variable β , but, in practice, the therapeutic decision remained unchanged because

Figure 2: Images in 48-year-old woman with complex cystic lesion of left breast. **(a)** B-mode US depicts a hypoechoic mass lesion with lobulated margins and slight posterior enhancement, classified as BI-RADS 4. **(b)** SSI shows no elasticity value for this lesion. Fine-needle aspiration was performed with US guidance, and a yellow liquid was evacuated. Final diagnosis was a cyst containing inflammatory cells and debris.

biopsy is also recommended for BI-RADS 4 lesions.

Discussion

Breast lesion detection and characterization at B-mode US is based mainly on specific description criteria defined by the American College of Radiology in the BI-RADS lexicon. For US descriptors, results of a prior study (18) showed that there is substantial agreement for lesion orientation, shape, and boundary ($\kappa = 0.61, 0.66, \text{ and } 0.69$, respectively), but

Figure 3: Images in 45-year-old woman with fibroadenoma. **(a)** B-mode US depicts a hypoechoic, homogeneous, lobular mass lesion classified as BI-RADS 3. **(b)** SSI shows a low elasticity score (<50 kPa).

for lesion margin and posterior acoustic features, the agreement is moderate ($\kappa = 0.40$ for both), and for lesion echo pattern, the agreement is poor ($\kappa = 0.29$). These description criteria often lead to false-positive findings and a number of unnecessary biopsies.

We have evaluated a quantitative elastography technique (ie, SSI) that could complement US examination in an efficient and easy-to-use way. The results of our preliminary work indicate that SSI was useful in demonstrating breast masses and characterizing cystic ones. This potential interesting application of SSI elastography relies on its capacity to reject cystic lesions, regardless of their typical or complicated B-mode US appearance, because of the

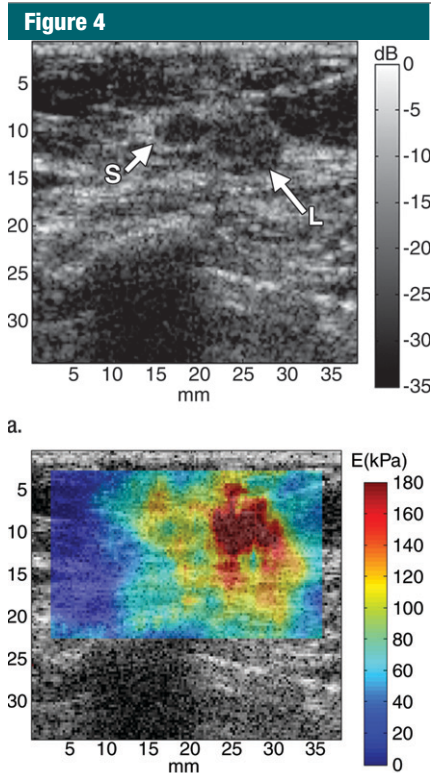


Figure 4: Images in 61-year-old woman already treated for breast cancer and referred because of suspicion of recurrence. **(a)** B-mode US depicts a 15-mm hypoechoic mass lesion (*L*) with irregular margins adjacent to the previous lumpectomy scar (*S*). This suspicious lesion was classified as BI-RADS 4. **(b)** SSI depicts a hard lesion ($E > 200$ kPa) highly suggestive of recurrence. The 90-kPa region on the left of this very stiff lesion corresponds to the scar. SSI depicted the two distinct neighboring zones of different elasticity (very stiff malignant lesion and moderately stiff scar). Biopsy results confirmed infiltrating ductal carcinoma.

absence of any shear wave propagation in liquid areas. During our preliminary study, no solid lesions presented a similar phenomenon of absence of shear wave propagation.

In solid, nonpalpable masses, quantitative elasticity may add potentially valuable information that could help radiologists better differentiate breast lesions. As already shown in the literature (8), less experienced radiologists, in particular, could be helped in their assessment by elasticity imaging. We believe that the SSI technique may have the potential to improve the decision about whether to

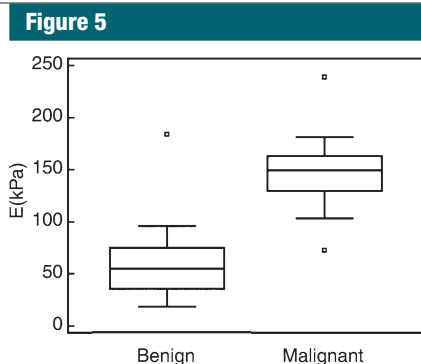


Figure 5: Box-and-whisker plot of Young modulus E estimated by using the SSI modality with respect to malignancy. According to the Mann-Whitney test, E values were significantly different between malignant and benign lesions ($P < .001$). Boxes = values from lower to upper quartiles, central lines = medians; whiskers extend from minimal to maximal values. Dots = outliers.

perform a percutaneous procedure such as biopsy or fine-needle aspiration.

From the user's perspective, one of the major differences of SSI compared with conventional elastography is that the mechanical vibration is induced automatically by the system by using the radiation force of ultrasound beams. The reliability of the imaging technique does not depend on the skills of the sonologist in correctly vibrating or stressing the tissue. The elasticity information is provided by using the same workflow and scanning conditions used for conventional B-mode US.

An interesting consequence is that the user does not need, as in conventional elastography, to subjectively or arbitrarily select one image in a complete image cine loop (7). With the SSI approach, a single set of successive US sequences provides a relevant elasticity image. Acquisition and postprocessing in our preliminary study on a dedicated research platform were limited by the slow transfer rate from electronics to personal computer boards and thus did not permit real-time elastography. However, no technologic issue prevents the SSI mode from providing elasticity images several times per second in the near future. In addition to conventional B-mode imaging, elasticity frame rates of three to four images per second are technologically feasible today.

The SSI approach also overcomes the intrinsic limitation of conventional elastography, which provides only qualitative and relative elasticity measurements. By providing local measurements of the true Young modulus of tissues across a wide stiffness range (from 1 to 240 kPa), SSI could be considered as a quantification tool for breast cancer diagnosis. Our results demonstrate that quantitative elasticity has clinical pertinence. The β variable, taking into account both the BI-RADS categorization and the Young modulus E , can ameliorate the overall diagnostic specificity (0.96 vs 0.63 for BI-RADS alone), whereas sensitivity remains high (0.95 vs 0.96 for BI-RADS alone). Larger clinical trials are necessary to validate these preliminary results.

Quantitative elasticity maps at SSI seem to allow finer assessment of tissue mechanical properties than does qualitative elastography by using external compression. At conventional elastography, the measured strain at one location depends on the surrounding tissues' mechanical properties. For example, a lesion having a softer center surrounded by a hard periphery would be impossible to detect because the whole lesion would move in a block under external stress. The local information provided by the SSI technique could lead to a much finer analysis of the spatial distribution and extension of tissue stiffness.

Our preliminary study had some limitations. All malignant lesions included in the study corresponded to infiltrating carcinomas, so we did not evaluate elasticity mapping in cases of ductal carcinoma in situ. Another limitation concerned the research platform used for SSI; our modified system was limited in terms of acquisition time, and B-mode images were substandard because of the 7.4-MHz array. This system was not capable of performing real-time SSI. Availability of real-time SSI quantitative elastography would be of great interest for evaluating mode robustness, reproducibility, and operator independence.

A major factor that remains to be understood is the effect of static

compression on the method. Human tissues have hardening properties; that is, their elasticity increases if static compression is applied. A study should be performed to quantify the influence of typical static compressions on the diagnostic value of the mode.

Our clinical investigation in 48 lesions showed that quantitative elasticity mapping of breast tissue is feasible in vivo by using the SSI method. Malignant lesions were significantly different from benign solid ones with regard to lesion elasticity quantitative value; because no shear wave propagation occurs in liquid areas, cystic lesions were diagnosed, regardless of their B-mode appearance. SSI could be a valuable complementary method for characterizing indeterminate breast lesions, thus obviating unnecessary biopsies. Large prospective trials are necessary to determine the role of SSI in a clinical setting.

Acknowledgments: The authors are grateful to Anne Badel, PhD, and Lilliane Ollvier, MD, for their essential contribution to this work.

References

1. Sewell CW. Pathology of benign and malignant breast disorders. *Radiol Clin North Am* 1995;33(6):1067-1080.
2. Tavassoli FA, Devilee P. Pathology and genetics: tumours of the breast and female genital organs. Lyon, France: IARC, 2003.
3. Garra BS, Cespedes EI, Ophir J, et al. Elastography of breast lesions: initial clinical results. *Radiology* 1997;202(1):79-86.
4. Hiltawsky KM, Krüger M, Starke C, Heuser L, Ermert H, Jensen A. Freehand ultrasound elastography of breast lesions: clinical results. *Ultrasound Med Biol* 2001;27(11):1461-1469.
5. Thomas A, Kümmel S, Fritzsche F, et al. Real-time sonoelastography performed in addition to B-mode ultrasound and mammography: improved differentiation of breast lesions? *Acad Radiol* 2006;13(12):1496-1504.
6. Itoh A, Ueno E, Tohno E, et al. Breast disease: clinical application of US elastography for diagnosis. *Radiology* 2006;239(2):341-350.
7. Burnside ES, Hall TJ, Sommer AM, et al. Differentiating benign from malignant solid breast masses with US strain imaging. *Radiology* 2007;245(2):401-410.
8. Scaperrotta G, Ferranti C, Costa C, et al. Role of sonoelastography in non-palpable breast lesions. *Eur Radiol* 2008;18(11):2381-2389.
9. Bercoff J, Tanter M, Fink M. Supersonic shear imaging: a new technique for soft tissue elasticity mapping. *IEEE Trans Ultrason Ferroelectr Freq Control* 2004;51(4):396-409.
10. Bercoff J, Tanter M, Muller M, Fink M. The role of viscosity in the impulse diffraction field of elastic waves induced by the acoustic radiation force. *IEEE Trans Ultrason Ferroelectr Freq Control* 2004;51(11):1523-1536.
11. Bercoff J, Chaffai S, Tanter M, et al. In vivo breast tumor detection using transient elastography. *Ultrasound Med Biol* 2003;29(10):1387-1396.
12. Tanter M, Bercoff J, Athanasίου A, et al. Quantitative assessment of breast lesion viscoelasticity: initial clinical results using supersonic shear imaging. *Ultrasound Med Biol* 2008;34(9):1373-1386.
13. Sarvazyan AP. Biophysical bases of elasticity imaging. In: *Acoustical imaging*. Vol 21. New York, NY: Plenum, 1995; 223-240.
14. American College of Radiology. *Ultrasound*. In: *Breast imaging reporting and data system (BI-RADS)*. 4th ed. Reston, Va: American College of Radiology, 2003.
15. U.S. Food and Drug Administration. Information for manufacturers seeking marketing clearance of diagnostic ultrasound system and transducers. <http://www.fda.gov/cdrh/ode/ulstran.pdf>. Published 1997. Accessed October 10, 2009.
16. Bercoff J, Criton A, Bacrie CC, et al. Shear-Wave™ Elastography: a new real time imaging mode for assessing quantitatively soft tissue viscoelasticity. *Proceedings of the 2008 IEEE International Ultrasonics Symposium*, Beijing, China, November 2-5, 2008.
17. Hanley JA, McNeil BJ. A method of comparing the areas under receiver operating characteristic curves derived from the same cases. *Radiology* 1983;148(3):839-843.
18. Lazarus E, Mainiero MB, Schepps B, Koelliker SL, Livingston LS. BI-RADS lexicon for US and mammography: interobserver variability and positive predictive value. *Radiology* 2006;239(2):385-391.